Electronic Supplementary Material (ESI) for Analyst.

Supporting Information for

Quantitative Imaging of the Sub-Organ Distributions of Nanomaterials in Biological Tissues via Laser Ablation Inductively Coupled Plasma Mass Spectrometry

Teerapong Jantarat, Joshua D. Lauterbach, Jeerapat Doungchawee, Dheeraj K. Agrohia, Richard W. Vachet*

Department of Chemistry, University of Massachusetts, 710 North Pleasant Street, Amherst, MA 01002, USA

*Corresponding author: rwvachet@chem.umass.edu

Table of Contents

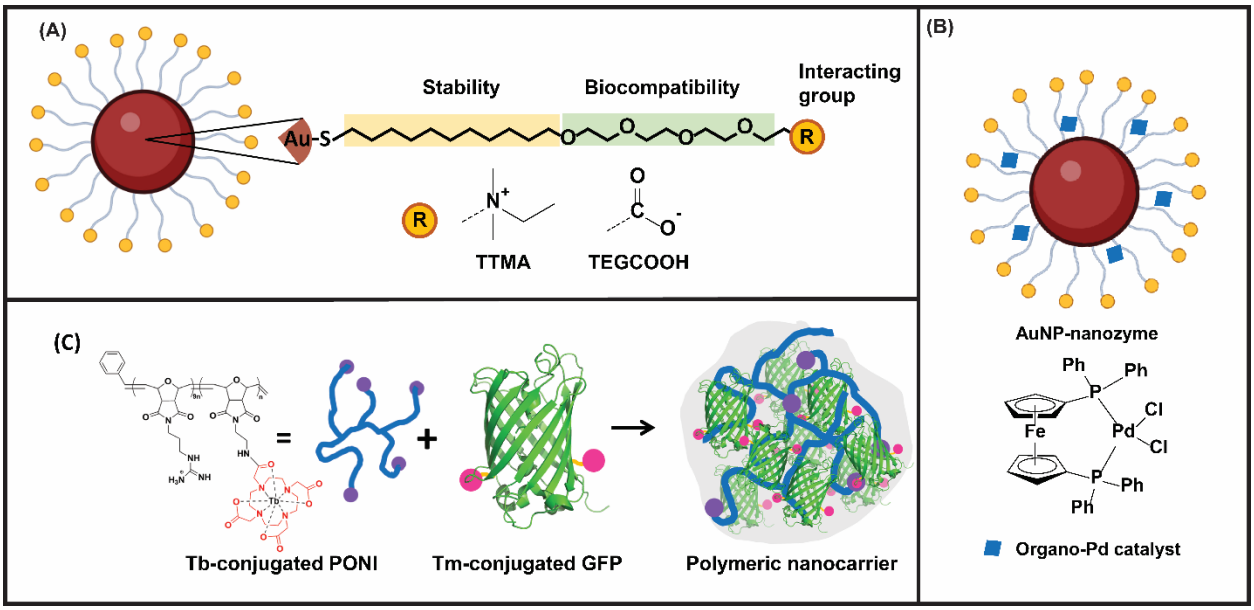

Figure S1. Nanomaterials used as model systems in this study. (A) Core-shell AuNPs consisting of a Au core with ~ 200 atoms coated with a monolayer of ligands that provides stability, biocompatibility, and an interacting group. (B) AuNP-nanozyme that are embedded with the indicated organo-Pd catalyst. (C) Polymeric-protein nanocomposites (PPNCs) that are composed of a guanidinium functionalized polyoxanorborneneimide (PONI) polymer and green-fluorescent protein (GFP) that are each separately conjugated with a DOTA ligand that binds Tb and Tm, respectively.

Table S1. Physical characteristics of the NMs used in this work as measured by DLS Malvern Zetasizer ZSP

NM type	Hydrodynamic Diameter (nm)	Zeta Potential (mV)
TTMA AuNPs	9.4 ± 0.4	+18.2 ± 1.3
TEGCOOH AuNPs	9.1 ± 0.1	-17.9 ± 1.4
Nanozyme	9.4 ± 0.4	+18.7 ± 2.2
polymeric NMs	1700 ± 300	+13.6 ± 1.2

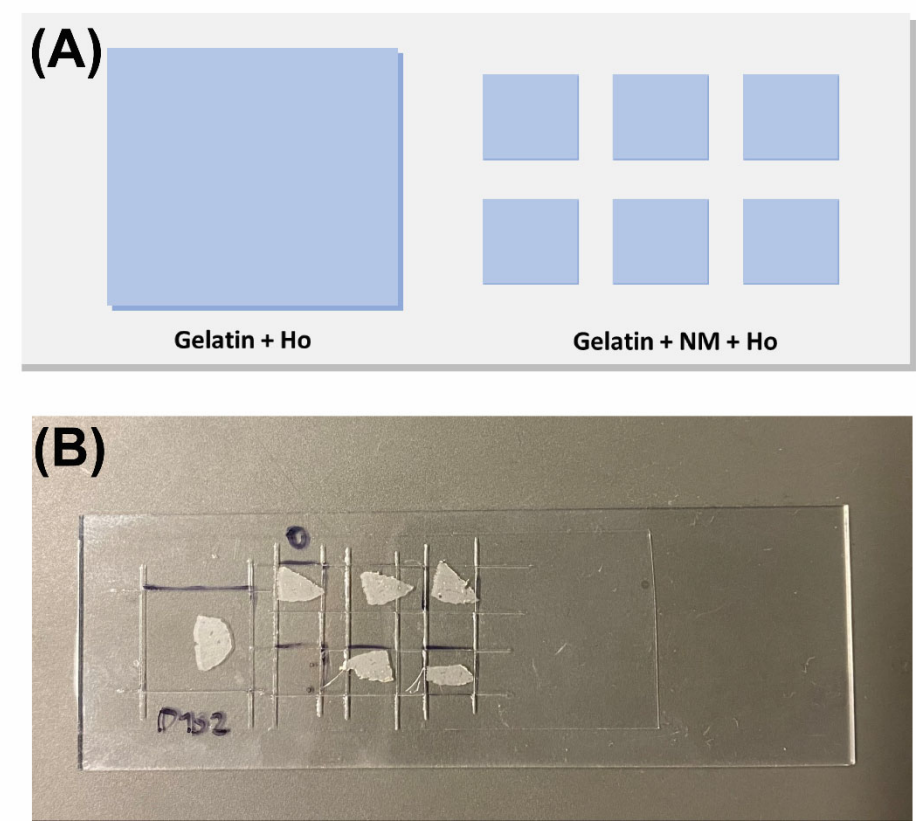

Figure S2. Schematic and picture of the mold used for preparation of the gelatin standards. (A) Illustration of the mold design. The large square area on the left is filled with Ho-spiked gelatin, upon which the tissue of interest would be placed. The remaining six smaller squares are filled with gelatin that is spiked with both the NM standards of interest and Ho as an internal standard. (B) A photograph of the prepared mold with the tissues placed on top of the spiked gelatin standards. The tissue of interest was placed on top of Ho-spiked gelatin in the large square, and control tissues were placed on top of the gelatin that was spiked with Ho and NMs at five different concentrations.

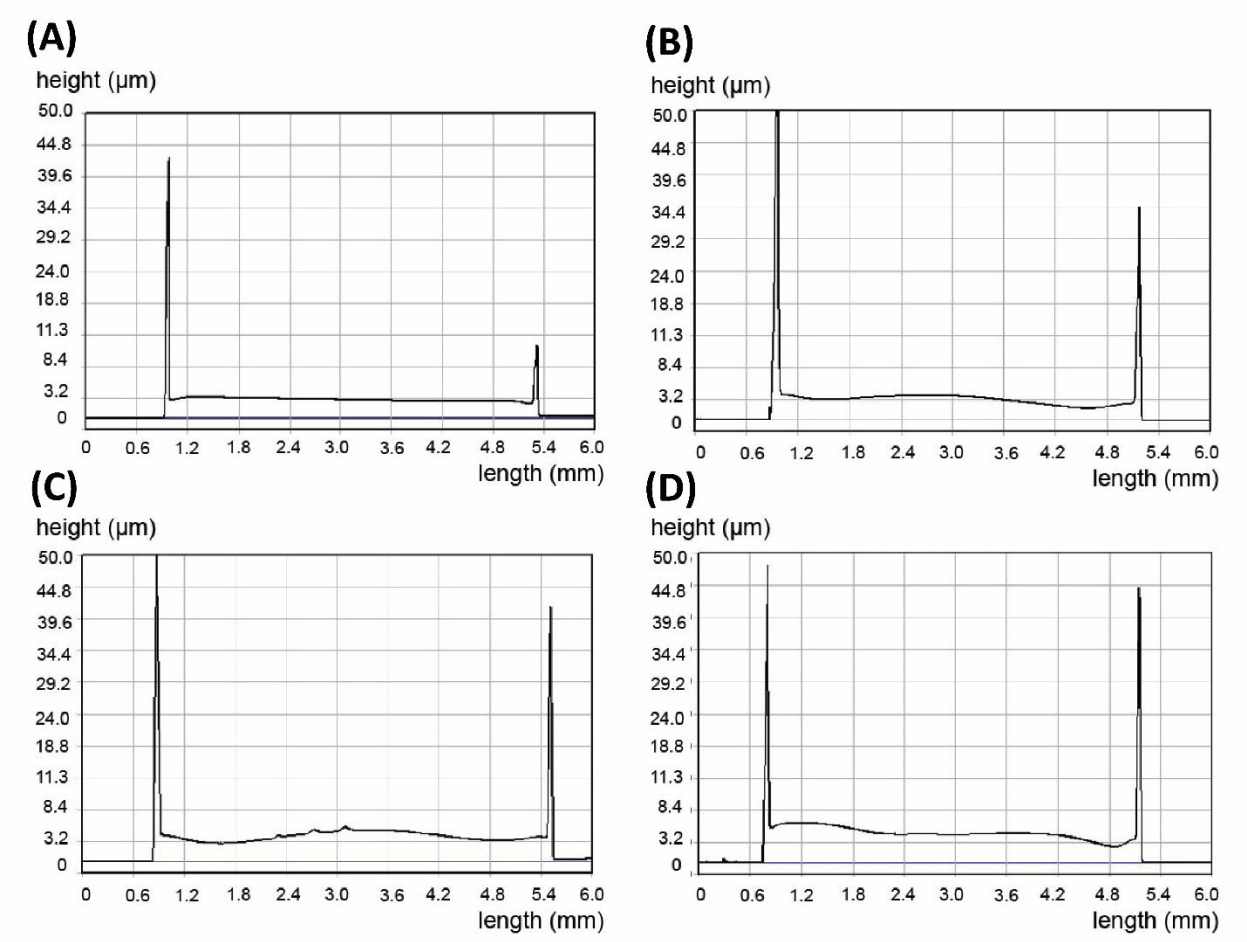

Figure S3. Thickness and surface roughness of the gelatin layers as measured by profilometry. Results for gelatin concentrations of (A) 7.5, (B) 10.0, (C) 12.5, and (D) 15.0 %w/v. The spikes at the edges of the plots result from when the Teflon tape was peeled off from the glass slide prior to the measurement, which causes the edges of the gelatin to be lifted. During standard and sample analyses tissues were not placed or analyzed near these edges.

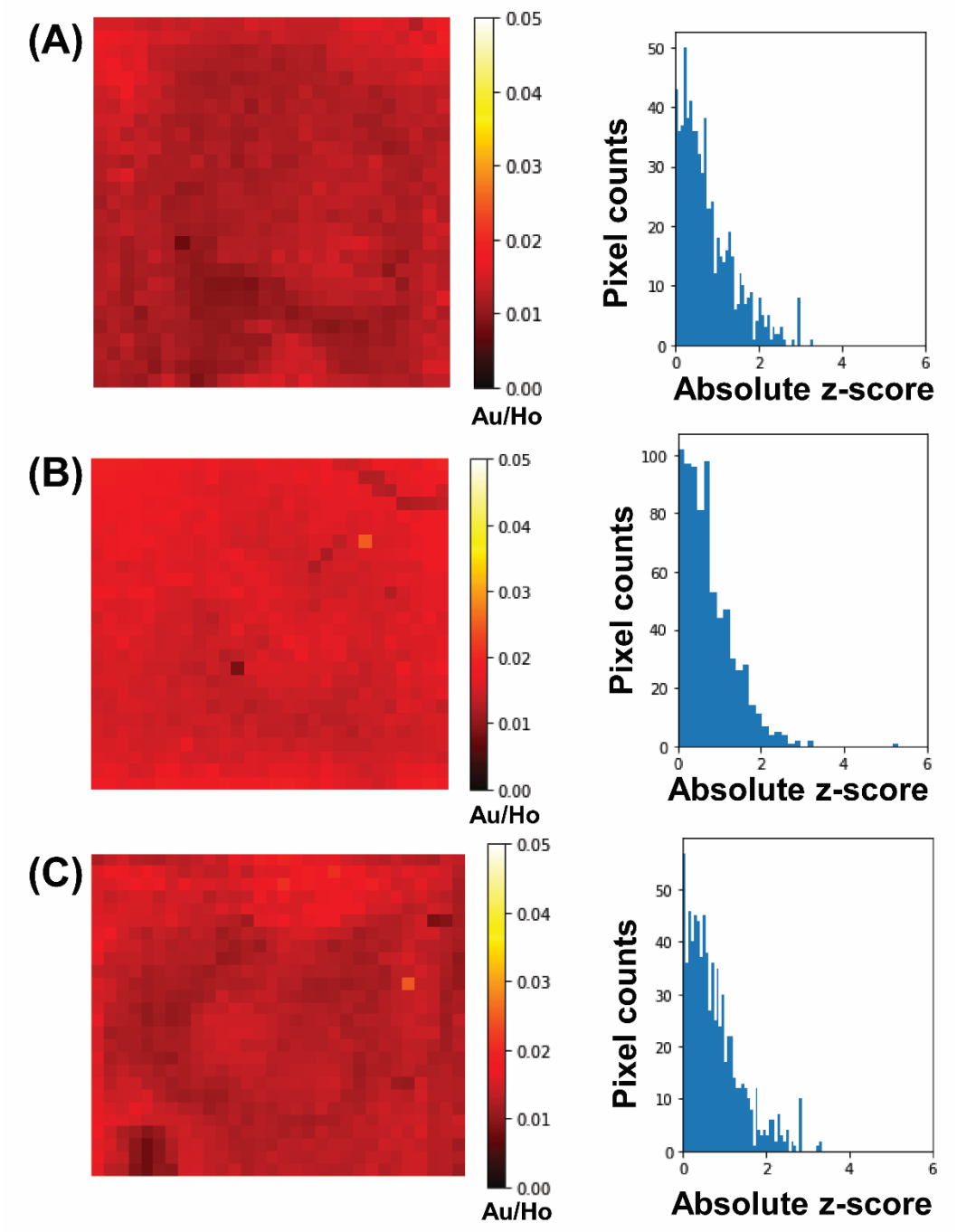

Figure S4. LA-ICP-MS images and z-scores of the normalized Au signal from 5 µM TTMA AuNPs spiked into gelatin containing 50 µg/g of the internal standard Ho at drying temperatures of (A) room temperature, (B) -20 ºC, and (C) 100 ºC. At each pixel, the Au signal was divided by the Ho signal. The absolute z-score represents the distribution of the pixel intensities in the images by reporting how many pixels are a given number of standard deviations away from the mean. More pixels with low z-scores indicate a more homogeneous distribution of signals.

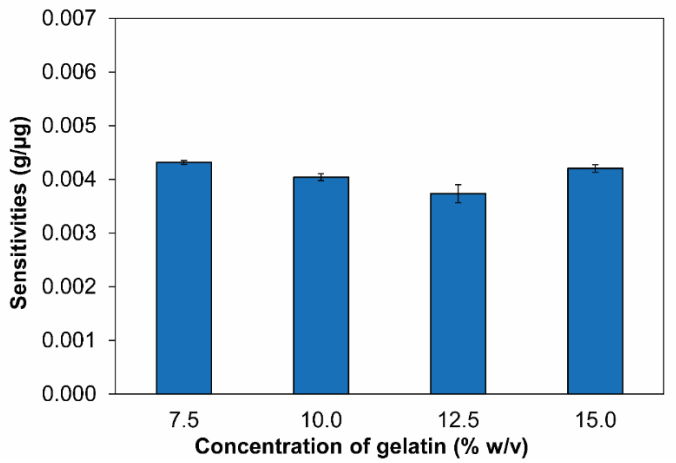

Figure S5. The optimum gelatin concentration was identified by varying concentrations from 7.5 to 15.0 % weight/volume (w/v). Sensitivities for the detection of Au were obtained from the slopes of the AuNP calibration plots at different gelatin concentrations. Each calibration was prepared using TTMA AuNPs in the range of 0 - 40 µg/g in gelatin, and Ho was spiked into the gelatin at 50 µg/g. The error bars represent the standard deviations from three replicate measurements.

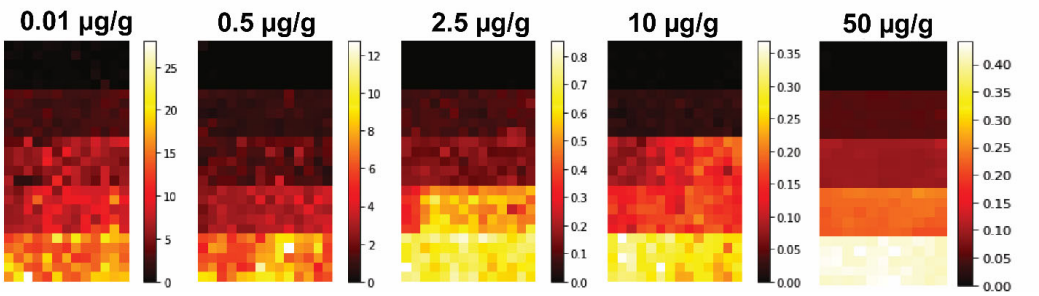

Figure S6. Normalized images of the calibration standards at different concentrations of Ho as an internal standard. In each condition, TTMA AuNPs were spiked into the gelatin at concentrations of 0, 5, 10, 20 and 40 µg/g. Ho was used as an internal standard and spiked into the gelatin. Ho concentrations were varied, as indicated above each image, and the normalized images were obtained by dividing the Au signal by Ho signal.

Table S2. Range of measured relative standard deviations (RSDs) obtained from the Au signal normalized to the Ho signal as shown in Figure S6.

Ho concentration	Range of RSD values[a]
0.01	10-31 %
0.5	17-35 %
2.5	9-25 %
10	10-32 %
50	2-10 %

[a] The RSD values were calculated from the signals of TTMA AuNPs (0, 5, 10, 20 and 40 µg/g) normalized to the indicate Ho concentration.

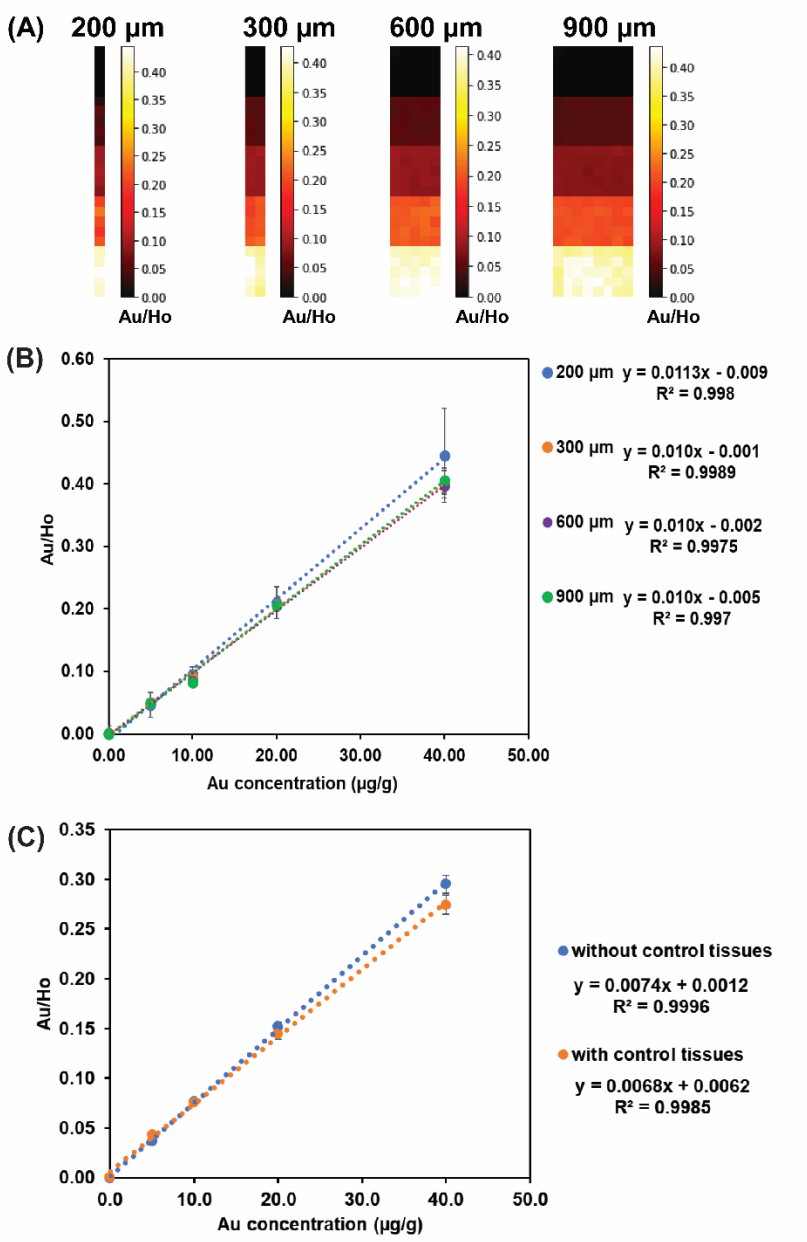

Figure S7. (A) The calibration standard images (Au/Ho) of gelatin spiked with increasing concentrations of TTMA AuNPs and Ho at 50 µg/g. Results were obtained from different ablation lengths of the spiked gelatin. (B) Calibration plots of Au/Ho vs. Au concentration for different ablation lengths. (C) Calibration plots of Au/Ho vs. Au concentration with and without control tissues on top of the gelatin standards. The error bars represent the standard deviation of the calibration standard images calculated based on all pixels in each standard concentration (i.e. those shown in Figure S7A).

Table S3. The total time required to acquire the data for the calibrations as a function of the ablated line length.

Length of ablated standard (μm)	Time required for one ablated line (s)	Total time required for the calibration (min)[a]
200	10	4.20
300	15	6.25
600	30	12.5
900	45	18.8

[a] For each standard concentration, five lines were ablated, and five concentrations of the standard (0-40 μg/g) were used to construct a calibration plot.

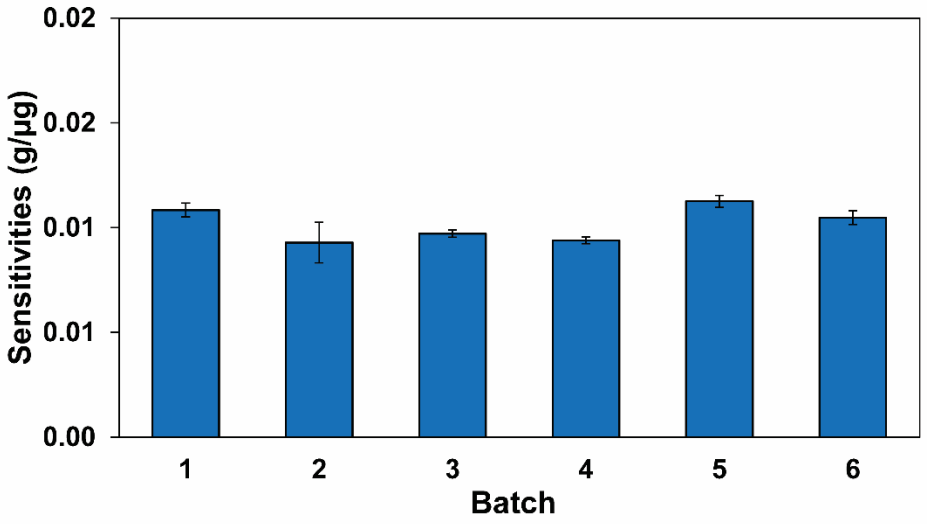

Figure S8. The reproducibility of the spiked gelatin standards is excellent as indicated by relatively little change in the calibration standard sensitivities. The sensitivities were obtained from the slopes of the calibration plots of six different batches of gelatin spiked with varying concentrations of TTMA AuNPs and 50 μg/g of Ho. These results were obtained over the period of two months. The error bars represent the standard deviations from three replicate measurements.

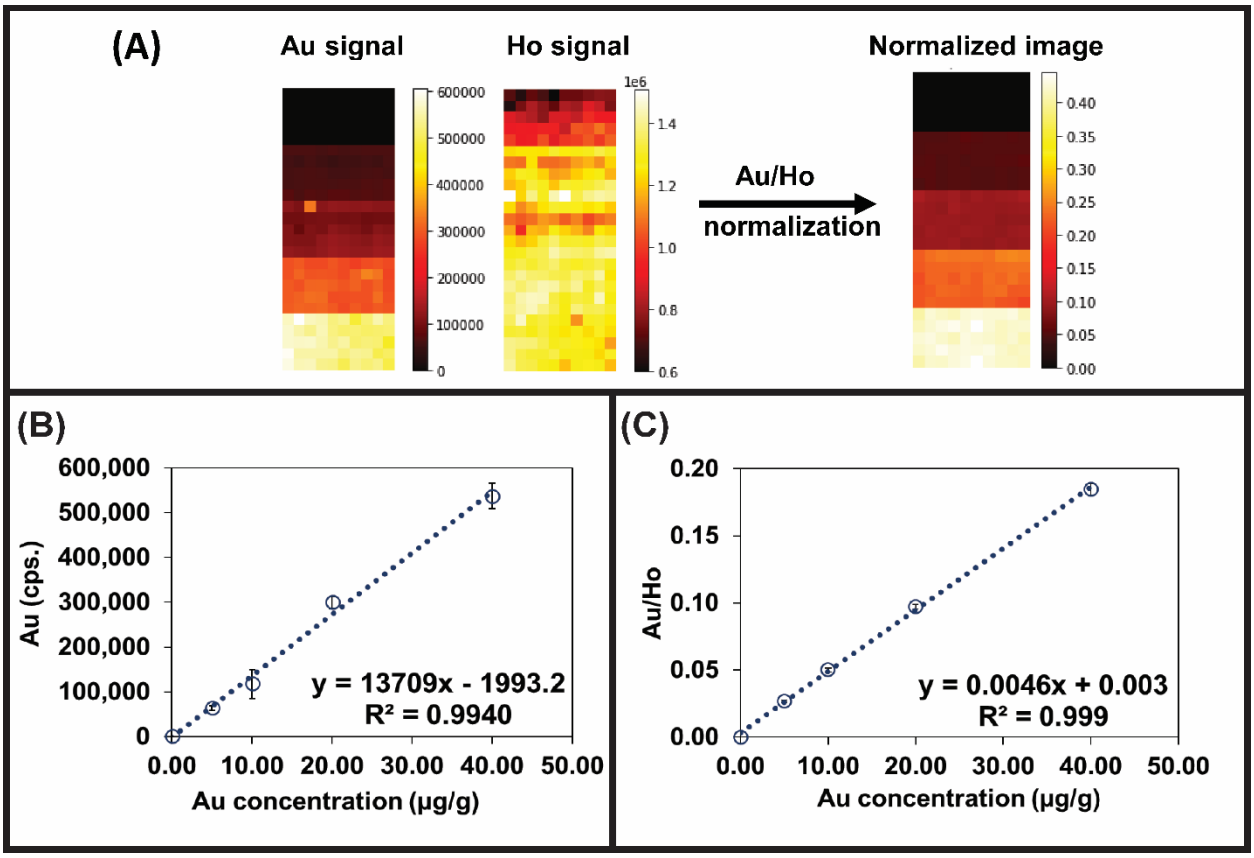

Figure S9. Normalization of the standard signals can correct for variations in laser energy during imaging. (A) Gelatin standards spiked with Ho (50 µg/g) as an internal standard and TTMA AuNPs with varying concentrations were prepared and analyzed by LA-ICP-MS under conditions in which the laser energy fluctuated. Normalization by dividing the Au signal by the Ho signal can correct for signal variations due to laser fluctuations. (B) Au calibration plot before normalization and (C) after normalization with Ho. The linearity of the calibration plot is improved (R^2 = 0.999) and the standard deviations are reduced (< 5.0 %) when Ho normalization is used.

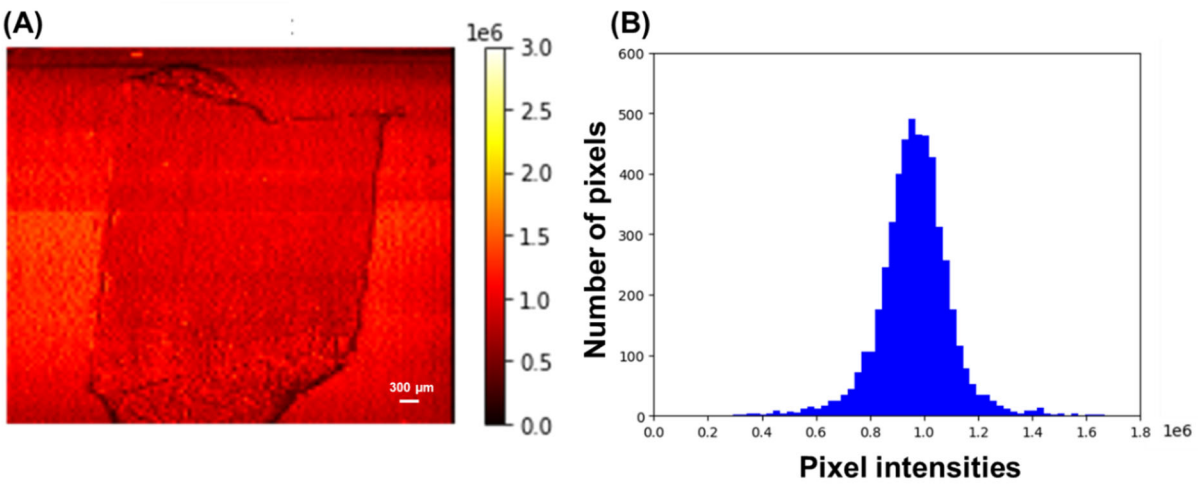

Figure S10. (A) An example of the homogenous distribution of Ho that is typically obtained in a gelatin layer underneath a tissue section (spleen in this case). Ho was spiked into the gelatin at 50 µg/g as an internal standard, and the spleen section from a mouse was placed on top of the spiked gelatin. The resulting LA-ICP-MS distribution of Ho is shown. (B) Histogram illustrating the distribution of pixels in the image in part (A).

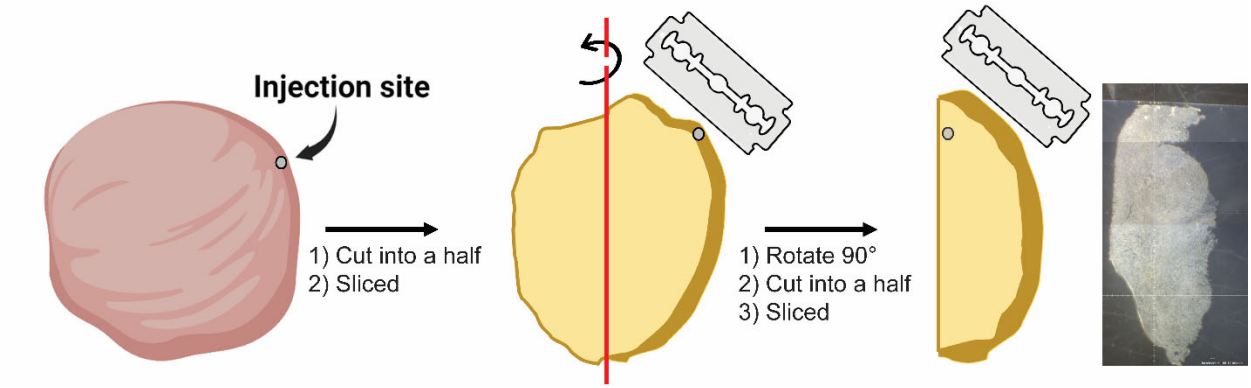

Figure S11. Illustration of how the tumor was sectioned. First, the tumor was cut in half, and then the tumor was sliced into multiple 12 µm sections for LA-ICP-MS imaging. After that, the same tumor was rotated 90° and cut into a half again before acquiring several more 12 µm sections. For all sections the injection site on the tumor was maintained.

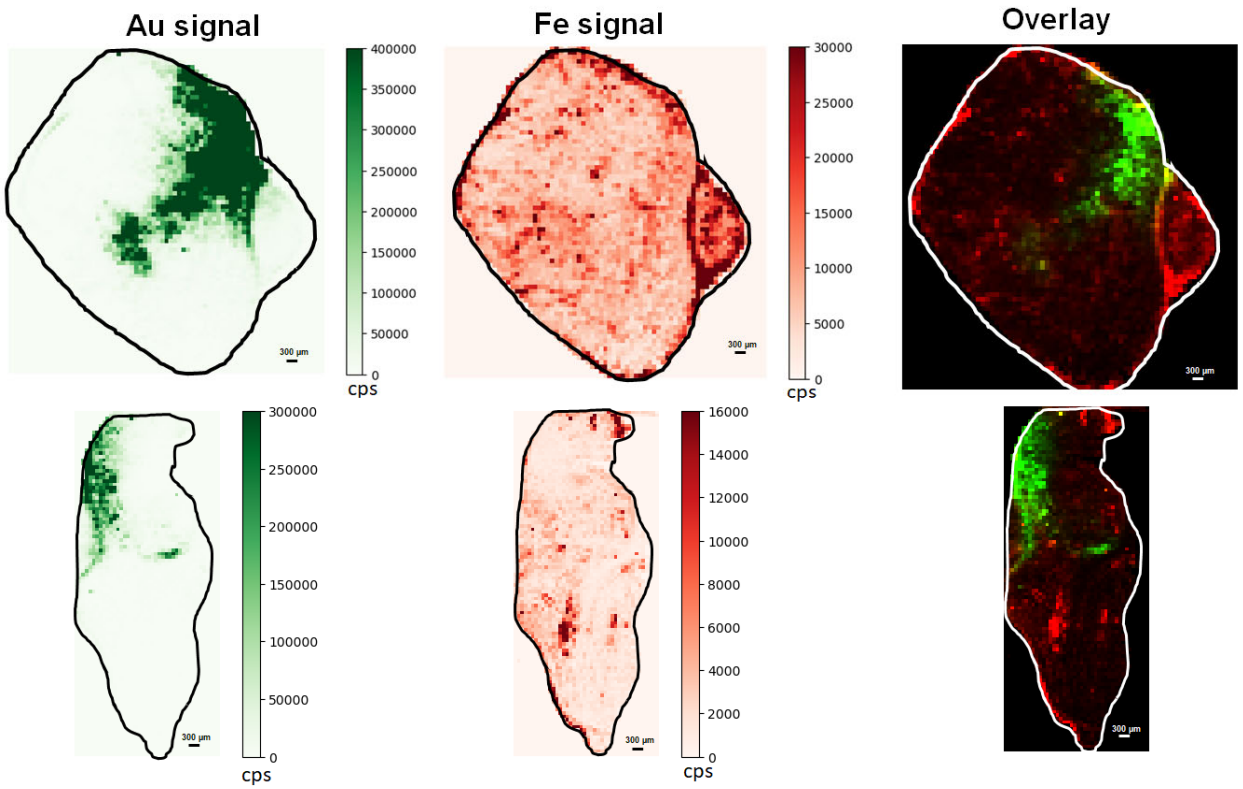

Figure S12. Au and Fe signal distributions and an overlay of the Au and Fe signals from LA-ICP-MS imaging of the two different tumor samples, with sections obtained as indicated in Figure S11. The tumor in the mouse was injected with the nanozyme, and the mouse was sacrificed 10 days after the injection.